Immobilized Fenton-Like Ionic Liquid: Catalytic Performance for Oxidative Desulfurization

Jun Xiong, Wenshuai Zhu, Huaming Li, Yehai Xu, Wei Jiang, Suhang Xun, and Hui Liu
School of Chemistry and Chemical Engineering, Jiangsu University, Zhenjiang 212013, P.R. China

Zhen Zhao
State Key Laboratory of Heavy Oil Processing, Faculty of Science, China University of Petroleum,
Beijing 102249, P.R. China

DOI 10.1002/aic.14197

MCM-41-supported Fenton-like ionic liquid catalysts were synthesized by the grafting method and applied in the removal of sulfur compounds in model oil. The structure and property of the catalysts were characterized by Fourier transform infrared spectra, X- ray diffraction, diffuse reflectance spectra, transmission electron microscopy, thermogravimetric and differential scanning calorimetry, and N_2 adsorption-desorption. Results suggested that Fenton-like ionic liquid was supported on mesoporous material MCM-41. Different desulfurization systems were studied. The results indicated that at room-temperature (30°C) for 1 h, MCM-41-supported Fenton-like ionic liquid in extraction combined with catalytic oxidative desulfurization (ECODS) system showed a high catalytic activity with H_2O_2 as the oxidant, and [Omim]BF_4 as the extractant. Different factors, such as temperature, the amount of H_2O_2, solvent, and different sulfur-containing compounds for sulfur removal were investigated. Through the gas chromatography-mass spectrometer (GC-MS) analysis, dibenzothoiphene sulfone was proved to be the only product of dibenzothiophene oxidizing reaction. Furthermore, the process of ECODS was confirmed by GC-MS results. © 2013 American Institute of Chemical Engineers *AIChE J*, 59: 4696–4704, 2013

Keywords: oxidative desulfurization, Fenton-like ionic liquid, supported catalyst, immobilization, mesoporous material

Introduction

During the last few decades, deep desulfurization of transportation fuels has been in need badly because of increasingly stringent regulations and fuel standards in many countries aiming to protect environment.[1] In view of the importance of desulfurization, several methods for desulfurization of fuels have been reported, such as hydrodesulfurization (HDS),[2,3] extraction,[4–6] adsorption,[7–9] oxidation,[10–13] and bioprocess.[14] HDS process has been used to eliminate sulfur compounds for industry purpose for the past few years; however, this method suffers from severe operating conditions (high temperature, high hydrogen pressure, and capital cost) and it is less effective for removing refractory sulfur compounds, such as benzothiophene (BT), dibenzothiophene (DBT), and their alky derivatives.[15] Among these methods, oxidative desulfurization (ODS) was considered as one of the most promising alternative technologies due to its advantages that many kinds of organic sulfur compounds can be removed effectively under the mild reaction conditions.[16,17] Generally, in the previous studies, most ODS reaction performed using homogeneous catalysis systems. The homogeneous catalysis has some drawbacks, such as, difficult separation or regeneration of catalysts and recontamination of oils from the dissolution of traces of catalysts.[18]

The heterogeneous catalysis can solve those problems aforementioned. The oxidation of sulfur compounds with heterogeneous catalysts systems has been studied such as mesoporous TiO_2,[19] HPWA-SBA-15,[20] and WO_x/ZrO_2.[21,22] Li et al.[23–25] investigated different supports with phosphotungstic acid, Ti-containing SBA-16-type mesoporous material,[26] and Fe-supported MCM-41 catalysts[27] for the oxidation of DBT with hydrogen peroxide as the oxidant. Yan et al.[28] reported mesoporous phosphotungstic acid/TiO_2 nanocomposite as a novel ODS catalyst. However, there are few research on supported ionic liquid catalysts for desulfurization.

In recent years, ionic liquids (ILs) as novel catalysts received particular interests, owing to their unique properties (e.g., thermal stability, negligible vapor pressure, and selective solubility). Task-specific ILs as catalysts have been exploited for ODS, such as, Fenton-like ILs,[16,29,30] metal-based surfactant-type ILs,[31] polyoxometalate-based ILs,[32,33] Brønsted acidic ILs,[18,34,35] and Lewis acidic ILs.[18,36] However, in the homogeneous catalysis systems, a large amount of ILs was needed. On the other hand, the high viscosity and cost of ILs restricted their industrial applications. Based on the economic criteria and industrial applications, immobilizing small amount of ILs on solid surfaces has been used as novel solid catalysts to solve this problem.

In previous studies, our group has applied Fenton-like ILs in ODS systems.[16,29,30] Although these Fenton-like ionic liquids presented high catalytic performance, they had some

---

Correspondence concerning this article should be addressed to H. Li at lihm@ujs.edu.cn.

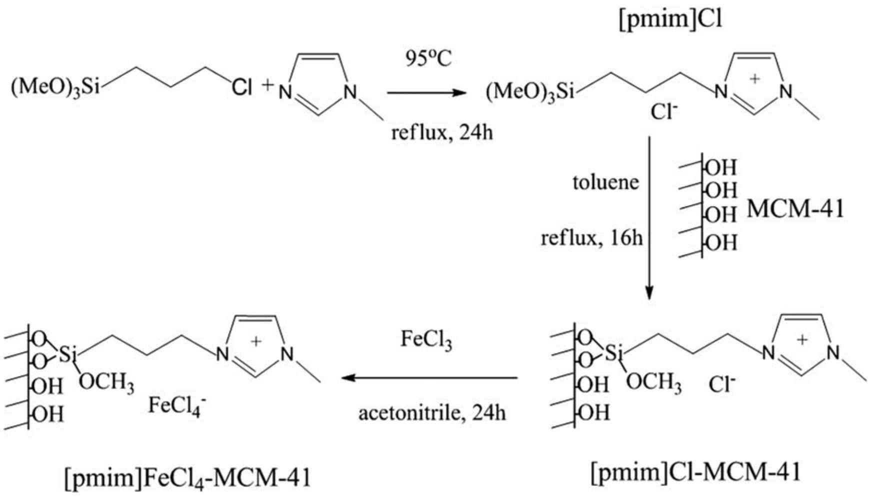

Scheme 1. Preparation of iron-based ionic liquid on the MCM-41.

problems, such as large amount of ILs wasted and the diesel contaminated. Inspired by previous work, we attempt to design a catalyst system immobilizing iron-based ILs on support. We chose MCM-41 as the support. MCM-41 is a mesoporous molecular sieve material, which consists of a hexagonal array of one-dimensional tunnel structure with highly specific surface, pore volume, and high thermal stability.[37] As catalyst supports, MCM-41 can provide the favorable space for the reaction of large molecules. In this study, to combine the advantages of MCM-41 and the appropriate activity of Fenton-like ionic liquid, we loaded chloroferrate (III) ionic liquid on MCM-41 by the grafting method. The aim of this research is to evaluate the ODS activity of heterogeneous catalysts of MCM-41-supported Fenton-like ionic liquid.

Experimental Section

Materials

BT, DBT, and 4,6-dimethyldibenzothiophene (4,6-DMDBT) were purchased from Sigma-Aldrich. Commercially available 33 wt % H_2O_2, iron (III) chloride anhydrous, *n*-dodecanethiol (DT), *n*-octane, tetradecane, and *N*-methylimidazole were purchased from Sinopharm Chemical Reagent. (3-chloropropyl)Trimethoxysilan (98%) was marketed by Aladdin Chemistry. The conventional ILs 1-butyl-3-methylimidazolium tetrafluoroborate ([Bmim]BF_4), 1-octyl-3-methylimidazolium tetrafluoroborate ([Omim]BF_4), 1-butyl-3-methylimidazolium hexafluorophosphate ([Bmim]PF_6), and 1-octyl-3-methylimidazolium hexafluorophosphate ([Omim]PF_6) were purchased from Shanghai Chengjie Chemical.

Catalyst preparation

1. Synthesis of 1-methyl-3-(trimethoxysilylpropyl)-imidazolium chloride ([pmim]Cl)

   The mixture of *N*-methylimidazole (freshly distilled) (10.3160 g, 0.1258 mol) and 3-chloropropyltrimethoxysilane (25 g, 0.1258 mol) was refluxed at 95°C for 24 h. After cooling to room-temperature, the reaction mixture was washed with diethyl ether and dried under vacuum.^{1}H NMR (400 MHz, DMSO): 9.81(s, 1H, NC*H*N), 8.12(d, 1H, CHC*H*NCH$_2$), 7.81(d, 1H, MeNC*H*CH), 4.26(t, 2H, NC*H$_2$*), 4.03(s, 3H, NC*H$_3$*), 3.92(s, 9H, O(*CH$_3$*)$_3$), 1.82(m, 2H, *CH$_2$*CH$_2$Si), 0.52(t, 2H, *CH$_2$*Si)
2. Grafting of 1-methyl-3-(trimethoxysilylpropyl)-imidazolium chloride ([pmim]Cl) on MCM-41([pmim]Cl-MCM-41)

   MCM-41 support was prepared according to the previous reports.[38,39] MCM-41 (2 g) was dispersed in 50-mL dried toluene and treated with 1-g [pmim]Cl. The mixture was heated under reflux (90°C) for 16 h. After cooling to room-temperature, the solid was isolated by filtration and dried under high vacuum. Then, the unreacted [pmim]Cl was removed by 48 h extraction with boiling dichloromethane. White powder of [pmim]Cl-MCM-41 was achieved under high vacuum.
3. Preparation of immobilized iron-based ionic liquid ([pmim]$FeCl_4$-MCM-41)

   [pmim]Cl-MCM-41 was stirred vigorously with $FeCl_3$ in acetonitrile at 83°C for 24 h. Then, the solid was isolated by filtration and washed with acetonitrile. The resulting solid was dried in vacuum to produce [pmim]-$FeCl_4$-MCM-41 ([pmim]Cl/ $FeCl_3$ molar ratios = 1:1.5). Scheme 1 depicts the synthesis process.

S1

Characterization

NMR spectra were recorded on Bruker AV-400 spectrometer (Germany) using dimethyl sulfoxide and $(CH_3)_4Si$ as the solvent and the reference, respectively. Chemical shifts (δ) were given in parts per million and coupling constants (J) in hertz.

Fourier transform infrared (FTIR) spectra were performed on a Nicolet FTIR spectrophotometer (Nexus 470, Thermo Electron Corporation) using KBr pellets at room-temperature.

Powder X-ray diffraction (XRD) analysis was carried out on Bruker D8 diffractometer with high-intensity Cu Kα ($\lambda = 1.54$ Å).

Thermogravimetric and differential scanning calorimetry (TG-DSC) was done on STA-449C Jupiter (NETZSCH Corporation, Germany). Sample weighing about 30 mg was heated from room-temperature to 1000°C at a heating rate 10°C/min in a dynamic N_2.

The diffuse reflectance spectra (DRS) were measured by a UV-vis spectrometer (UV-2450, Shimadzu) in the range of 200–800 nm. $BaSO_4$ was used as the reflectance standard material.

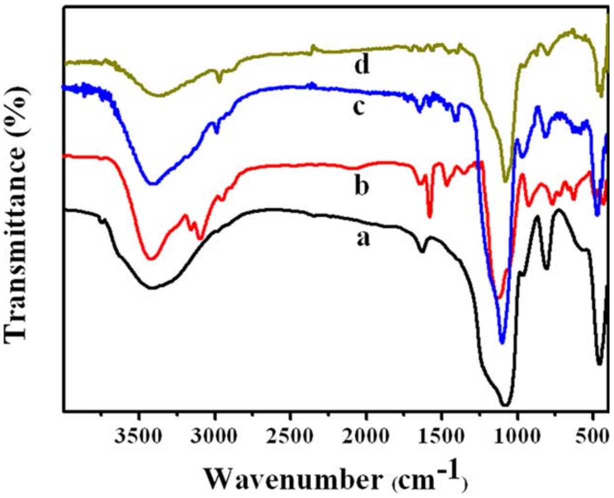

Figure 1. FTIR spectra of MCM-41(a), [pmim]Cl(b), [pmim]Cl-MCM-41(c), and [pmim]FeCl$_4$-MCM-41(d).

[Color figure can be viewed in the online issue, which is available at wileyonlinelibrary.com.]

Transmission electron microscopy (TEM) micrographs were taken with a JEOL-JEM-2010 (JEOL, Japan) operating at 200 kV. The samples used for TEM were prepared by dispersing some products in ethanol, then placing a drop of the solution onto a copper grid, and letting the ethanol evaporate slowly in air.

The N$_2$ adsorption–desorption isotherms at 77 K were investigated using a TriStar II 3020 surface area and porosity analyzer (Micromeritics Instrument).

ODS process

Model oil was prepared by dissolving DBT, BT, 4,6-DMDBT, and DT in *n*-octane, with a corresponding S-content of 500, 250, 250, and 250 ppm, respectively. Desulfurization was carried out in a home-made 40-mL two-necked flask. After catalyst, conventional IL, model oil were added to the flask in turn, 33 wt % H$_2$O$_2$ was added into the mixture, and then the mixed solution was stirred vigorously at 30°C for 1 h.

Analysis methods

The remaining sulfur-containing compounds in model oil after the reaction were analyzed by Gas Chromatography-Flame Ionization Detector (GC-FID) with tetradecane with tetradecane as the internal standard. (Agilent 7890A; HP-5, 30 m × 0.32 mm i.d. × 0.25 μm; FID: Agilent). The conversion of DBT in the model oil was used to calculate the removal of sulfur compounds.

The oxidized S-compound was characterized by Gas Chromatography-Mass Spectrometer (GC-MS) (Agilent 7890/5975C-Gas Chromatography(GC)/Mass Selective Detector (MSD); HP-5 MS column, 30 m × 250 μm i.d. × 0.25 μm; temperature program: 100°C-temperature rising 15°C/min-200°C for 10 min).

Results and Discussion

Catalyst characterization

FTIR spectra of MCM-41, [pmim]Cl, [pmim]Cl-MCM-41, and [pmim]FeCl$_4$-MCM-41 are shown in Figure 1. The Si—O—Si characteristic peaks of MCM-41 could be observed at 1079, 808, and 458 cm^{-1}. And a broad, asymmetric feature was seen at 3416 cm^{-1} belonging to O—H vibrations of silanols and water in mesoporous silica MCM-41. The absorption peaks at 1569 and 1630 cm^{-1} were assigned to C=N and C=C vibrations of the imidazole ring, which confirmed that there was the formation of [pmim]Cl. Additional bands at 3146, 3089, 2938, 1450, 915, 758, and 715 cm^{-1} were attributed to C—H stretching and deformation vibrations of the imidazole part and alkyl chain. The main characteristic peaks of MCM-41 and [pmim]Cl could be observed in the FTIR spectrum of [pmim]Cl-MCM-41 and [pmim]FeCl$_4$-MCM-41, which identified the presence of Fenton-like ionic liquid in MCM-41.

The low-angle XRD patterns of MCM-41 and [pmim]-FeCl$_4$-MCM-41 are depicted in Figure 2. MCM-41 pattern showed an intense reflection at $2\theta = 2.14°$ for d_{100} and two other weaker peaks at $2\theta = 3.68°$ and $2\theta = 4.24°$ for d_{110} and d_{200}, respectively, indicating the quasiregular arrangement of mesopores with hexagonal symmetry.[40] [pmim]FeCl$_4$-MCM-41 displayed decreased intensities of all the peaks and the diffraction peaks shifted to higher angles. This was attributed to that the ionic liquid moieties were inside the mesoporous channels of MCM-41, leading to decrease local order of MCM-41. However, the mesoporous structure of MCM-41 remained integrity during the immobilized process.

Figure 3 displays the diffuse–reflectance UV-vis spectroscopy of MCM-41, [pmim]Cl-MCM-41, and [pmim]FeCl$_4$-MCM-41. MCM-41 exhibited characteristic absorption bands in UV region.[41] It was found that the absorption band of [pmim]Cl-MCM-41 was at about 200–250 nm. In the case of [pmim]FeCl$_4$-MCM-41, the absorption region extended to about 500 nm. The 3d energy orbitals of Fe^{3+}, which is equal to each other, split from five degenerate orbitals with the same energy level into several d-orbitals with different energy when combined with Cl$^-$ ions to form clathrate with some kind of space structure in the electric field of ligand Cl$^-$. So that, the d-d transition absorption belts mainly appeared in the visible and ultraviolet region.

The transmission electron microscopy (TEM) images of MCM-41 and [pmim]FeCl$_4$-MCM-41 are shown in the

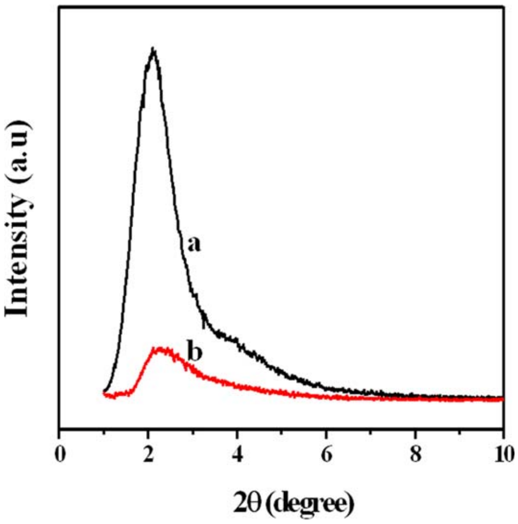

Figure 2. Low-angle XRD of MCM-41 (a) and [pmim] FeCl$_4$-MCM-41 (b).

[Color figure can be viewed in the online issue, which is available at wileyonlinelibrary.com.]

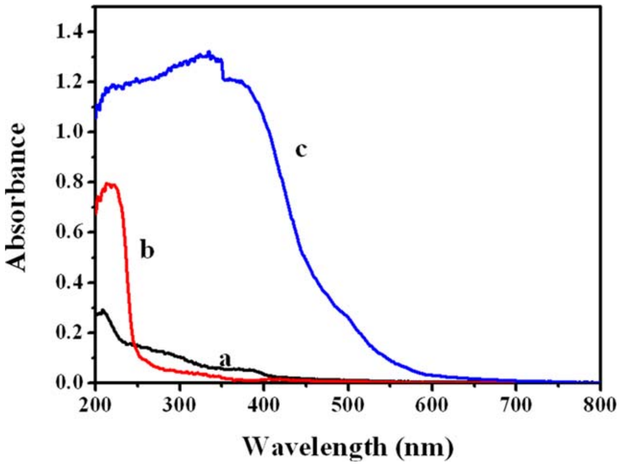

Figure 3. DRS spectra of MCM-41(a), [pmim]Cl-MCM-41(b), and [pmim]$FeCl_4$-MCM-41(c).

[Color figure can be viewed in the online issue, which is available at wileyonlinelibrary.com.]

Figure 4. The results indicated that the TEM images of MCM-41 (Figure 4a) and [pmim]$FeCl_4$-MCM-41 (Figure 4b) exhibited similar structure, which provided strong evidence that the mesoporous structure of support was retained after grafted Fenton-like ionic liquid.

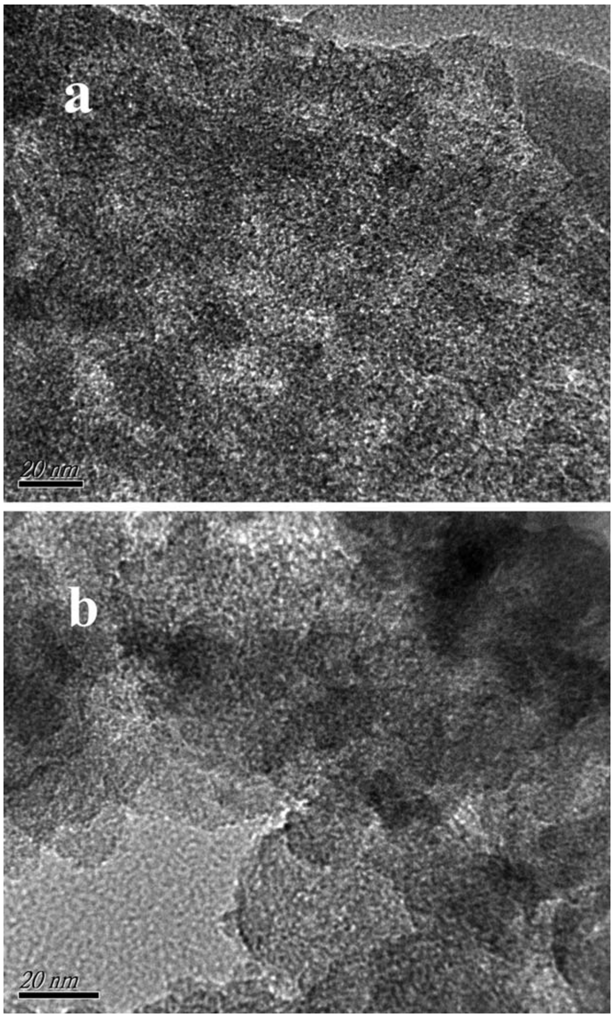

Figure 4. TEM image of (a) MCM-41 and (b) [pmim]-$FeCl_4$-MCM-41.

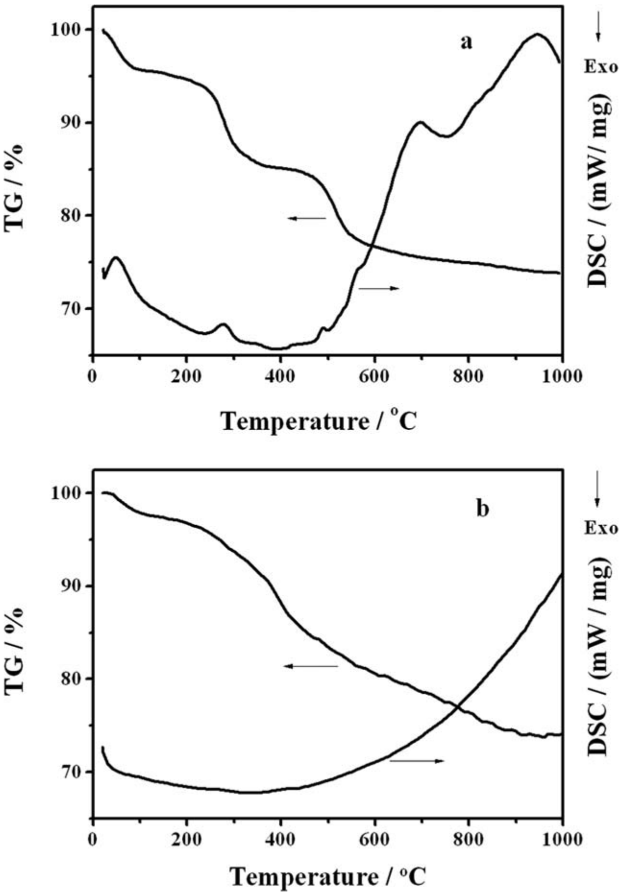

Figure 5. TG-DSC of [pmim]Cl-MCM-41 (a) and [pmim]-$FeCl_4$-MCM-41 (b).

The thermal stability of [pmim]Cl-MCM-41 and [pmim]-$FeCl_4$-MCM-41 is characterized by TG-DSC (Figure 5). Three major weight losses were observed at the TG-DSC curve of [pmim]Cl-MCM-41 (Figure 5a). The corresponding endothermic peak on DSC curve emerged below 100°C in the first step, which demonstrated the desorption of physically absorbed water. For the second weight loss between 170 and 340°C, it was attributed to the decomposition of the hydrogen-bonding networks. Above 430°C, there was a mass loss on TG curve. The reason may be that immobilized imidazole ionic liquid was destroyed. The TG-DSC curves of [pmim]$FeCl_4$-MCM-41 are given with a similar decomposition process (Figure 5b).

N_2 adsorption–desorption isotherms and the Barrett-Joyner-Halenda (BJH) pore-size distribution curves of MCM-41, [pmim]Cl-MCM-41, and [pmim]$FeCl_4$-MCM-41 are depicted in Figure 6. The samples displayed type IV isotherms and capillary condensation at relative pressures of $0.3 < P/P_0 < 0.5$, which was the characteristic of mesoporous materials. The textural properties of MCM-41 were substantially maintained after immobilization of imidazolium ionic liquid and on subsequent anchoring of $FeCl_3$. The surface area, pore volume, and pore diameters of MCM-41, [pmim]Cl-MCM-41, and [pmim]$FeCl_4$-MCM-41 are listed in Table 1. The MCM-41 sample exhibited a maximum pore volume (1.18 cm^3/g) and surface area (955 m^2/g). [pmim]Cl-MCM-41 resulted in a shift of the pore maximum to smaller volume (0.68 cm^3/g) and a decrease in surface area (547 m^2/g).

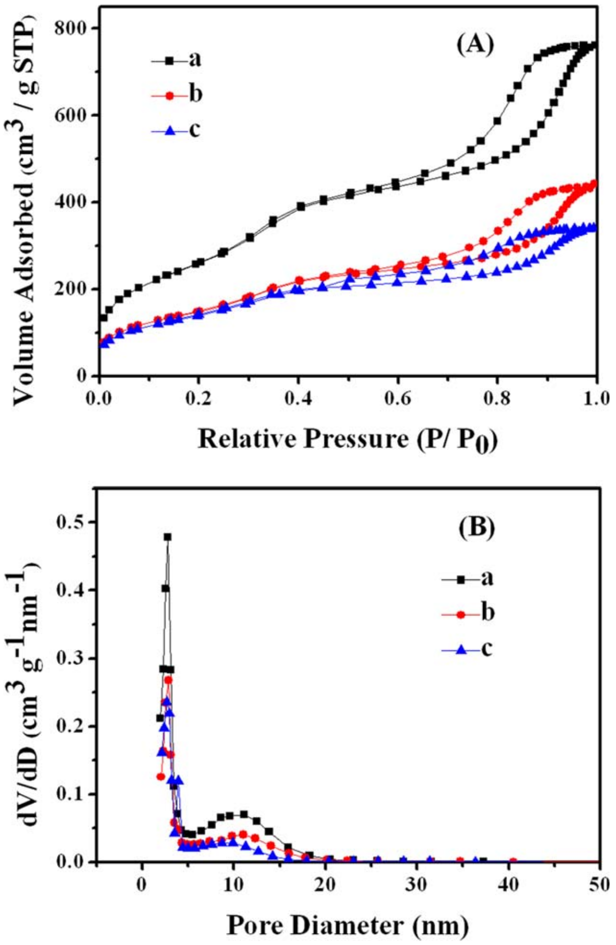

Figure 6. N_2 adsorption-desorption isotherms (A) and the BJH pore-size distribution curves (B) of MCM-41(a), [pmim]Cl-MCM-41(b), and [pmim]$FeCl_4$-MCM-41(c).

[Color figure can be viewed in the online issue, which is available at wileyonlinelibrary.com.]

The introduction of $FeCl_3$ led to a further decrease in surface and pore volume. It could be concluded that introduction of Fenton-like ionic liquid significantly affected the surface area and pore volume of the support.

Influence of different desulfurization systems on removal of DBT

The desulfurization activities of different systems are investigated in Table 2, including adsorption, catalysis combined with chemical oxidation, extraction, extraction coupled with chemical oxidation, and extraction combined with catalytic oxidation. In adsorption systems, when using mesoporous support MCM-41 solely as the adsorbent for removing DBT in model oil, the sulfur removal could reach 12.7% (Table 2, Entry 1), whereas for [pmim]$FeCl_4$-MCM-41, the sulfur removal only was 9.1% (Table 2, Entry 2). The reason for the lower adsorbability might be that the surface area of [pmim]$FeCl_4$-MCM-41 was smaller than that of MCM-41 (Table 1).

Table 1. The structure Properties of the Samples

Sample	S_{BET} (m^2/g)	Pore Volume (cm^3/g)	Pore Size (nm)
MCM-41	955	1.18	4.4
[pmim]Cl-MCM-41	547	0.68	4.5
[pmim]$FeCl_4$-MCM-41	515	0.53	4.0

Table 2. Comparison of Different Desulfurization Systems on Removal of DBT in Model Oil[a]

Entry	Desulfurization System	Sulfur Removal[b] (%)
1	MCM-41	12.7
2	[pmim]$FeCl_4$-MCM-41	9.1
3	MCM-41 + H_2O_2	8.7
4	[pmim]$FeCl_4$-MCM-41 + H_2O_2	11.8
5	[Omim]BF_4	34.5
6	[Omim]BF_4 + H_2O_2	36.7
7	[pmim]$FeCl_4$-MCM-41+H_2O_2 + [Omim]BF_4	91.6
8	MCM-41 + H_2O_2 + [Omim]BF_4	38.7
9[c]	1.5$FeCl_3$/MCM-41 + H_2O_2 + [Omim]BF_4	38.1

Experimental conditions: 5-mL model oil, 0.39-mmol H_2O_2, 1-mL [Omim]BF_4, 30°C, 1-h.
[a] m (catalyst) = 0.06 g.
[b] Max error = ±3%.
[c] m (catalyst) = 0.0231g.

With addition of H_2O_2 in MCM-41, the sulfur removal decreased to 8.7% (Table 2, Entry 3). The lower S-removal could be due to hydrophilic channels of the MCM-41 structure. MCM-41 absorbed easily the polar molecules H_2O_2 and reduced the capability to absorb the weak polarity compounds such as DBT.[42–44] Meanwhile, it could be concluded that MCM-41 could not activate hydrogen peroxide. Under the same reaction conditions, [pmim]$FeCl_4$-MCM-41 also showed low activity (Table2, Entry 4), which could be due to severe H_2O_2 self-decomposition.

When [Omim]BF_4 was used as the extractant to remove DBT from model oil, the desulfurization efficiency was also not high (34.5% sulfur removal). The sulfur removal increased to 36.7% with addition of H_2O_2 in [Omim]BF_4. In the case of the extraction combined with catalytic oxidative desulfurization (ECODS) system composed of [Omim]BF_4, [pmim]$FeCl_4$-MCM-41, and H_2O_2, the sulfur removal of DBT increased sharply (91.6%). It clearly demonstrated that, the ECODS system, which was composed of [Omim]BF_4, H_2O_2, and [pmim]$FeCl_4$-MCM-41, showed excellent performance for oxidation of DBT.

From the results in Entry 7, 8, it can be seen that [pmim]-$FeCl_4$-MCM-41 presented much higher activity than MCM-41 under the ECODS system. 1.5$FeCl_3$/MCM-41 with the same Fe content (Table 2, Entry 9) was also examined under the same reaction system, and poor desulfurization was found (sulfur removal was only 38.1%), indicating that the catalytic activity was not the result of $FeCl_3$ and that the existence of the immobilized imidazolium groups was essentially important for desulfurization reaction.

Influence of different reaction parameters on sulfur removal

The effect of reaction parameters, such as temperature, the amount of oxidizing agent, and solvent on oxidation of DBT were studied using the [pmim]$FeCl_4$-MCM-41 as the catalyst (Table 3).

The results of the effect of temperature on DBT conversion are presented in Table 3, Entries 1–3. At higher temperature (40°C, 50°C), although the H_2O_2/DBT molar ratio was 5:1 (excess oxidant), possibly due to more H_2O_2 decomposed with the increasing temperature, DBT conversion did not increase, which led to the worse utilization of H_2O_2. There

Table 3. Reaction Parameter in [pmim]$FeCl_4$-MCM-41Catalyzed Oxidative Desulfurization

Entry	Temperature (°C)	n (H_2O_2/DBT)[a]	Solvent	Sulfur Removal[b](%)
1	30	5	[Omim]BF_4	91.6
2	40	5	[Omim]BF_4	89.9
3	50	5	[Omim]BF_4	83.3
4	30	4	[Omim]BF_4	90.5
5	30	5	[Omim]BF_4	91.6
6	30	6	[Omim]BF_4	88.7
7	30	5	[Bmim]BF_4	86.6
8	30	5	[Omim]BF_4	91.6
9	30	5	[Bmim]PF_6	24.4
10	30	5	[Omim]PF_6	47.8

Experimental conditions: 5-mL model oil, 0.06-g catalyst, 1-mL solvent, 1 h.
[a] Molar ratio.
[b] Max error = ±3%.

exist two parallel reactions: catalytic oxidation and thermal decomposition of H_2O_2. Therefore, it is favorable to conduct the oxidation of DBT over immobilized [pmim]$FeCl_4$-MCM-41 at low temperatures, such as 30°C.

The desulfurization reactions under various H_2O_2/DBT molar ratios were carried out at 30°C for 1 h (Table 3, Entries 4-6). The optimal value of H_2O_2/DBT molar ratio was 5:1 (0.39 mmol H_2O_2), which was higher than the value of stoichiometric H_2O_2/DBT molar ratio for oxidation of DBT to dibenzothiophene sulfone ($DBTO_2$). This result may be restricted by two factors: the surplus amount of oxidant promoted the equilibrium reaction; on the other hand, the thermal decomposition of oxidant and oxidation reaction produces water, which inhibits the ODS reactions.[45] Therefore, H_2O_2/DBT molar ratio of 5:1 can improve ODS activity of sulfur compounds in the reaction system.

Solvents have a great influence on the catalytic ability of the supported Fenton-like ionic liquid catalyst. In constrained environment, conventional ILs were chosen as reaction solvents. The results (Table 3, Entries 7–10) showed higher activity in the case of [Omim]BF_4 (91.6 %), followed by [Bmim]BF_4 (86.6%), [Omim]PF_6 (47.8%), and [Bmim]PF_6 (24.4%), with 0.39 mmol H_2O_2 and 30°C. The activity of the catalyst was found to depend on the nature of the solvents. Various cations and anions may influence the properties of the ILs. In this study, the alkyl part $[Omim]^+$, as well as anion BF_4^- had a significant effect on desulfurization removal. Meanwhile, it was observed that H_2O_2 in ILs with PF_6^- decomposed violently in the experimental process. The result and observation confirmed that ILs with BF_4^- could prevent H_2O_2 from decomposing. At the same time, it was reported that ILs with longer alkyl chains showed higher extraction desulfurization removal.[15] Thus, when ILs with the same anion, $[Omim]^+$ had higher desulfurization removal than $[Bmim]^+$. Therefore, [Omim]BF_4 was selected and used in desulfurization reaction.

Influence of different molar ratios of [pmim]Cl to $FeCl_3$ on sulfur removal

To investigate the effect of molar rate of [pmim]Cl to $FeCl_3$ on DBT oxidation, immobilized catalysts were prepared with various molar ratios $FeCl_3$ ($n = 1$, 1.5, 2, 3) on mesoporous material and tested in desulfurization (Table 4). The lower activity of n ([pmim]Cl:$FeCl_3$) = 1:1 could be due to a lower molar fraction $FeCl_3$. It has been reported that the Lewis acidity of the iron-containing ILs can be modified by varying the fraction of $FeCl_3$. In other words, a higher molar fraction of $FeCl_3$ can lead to stronger Lewis acidity of $FeCl_3$-based IL.[46] With an increase in molar fraction of $FeCl_3$, DBT conversion exhibited a slight increase. At higher loading, the aggregation of Fenton-like ionic liquid lowered the dispersion of active sites. n ([pmim]Cl:$FeCl_3$) = 1.5 showed the higher activity (DBT conversion of 91.6%) and could achieve the aim of the deep desulfurization; thus, this was used in the following investigation.

Sulfur removal of different sulfur-containing compounds

The catalytic performance of [pmim]$FeCl_4$-MCM-41 was investigated by extraction combined with catalytic oxidation of other sulfur compounds besides DBT, including BT, DT, and 4,6-DMDBT under the given conditions. The results are shown in Figure 7. From the data, it can be seen that the sulfur removal decreased in following order: DBT > DT > BT > 4,6-DMDBT at 30°C for 1 h. As the reaction went on, the sulfur removal could reach around 90% for DBT and DT. This result demonstrated that the intrinsic properties of the sulfur-containing compounds were a critical factor for desulfurization reaction. These differences mainly came from three factors, that was, aromatic π-electron density of sulfur compounds, compound types, and molecular size. First, compared with aromatic compounds, aliphatic compounds were oxidized easily. Therefore, DT exhibited the higher sulfur removal. In the case of aromatic sulfur compounds, the electron density on the sulfur atom of DBT, BT, and 4,6-DMDBT is 5.758, 5.739, and 5.760, respectively.[47] For DBT and BT, the desulfurization performance increased with the aromatic π-electron density increased. On the other hand, in mesoporous environment, it could be difficult for macromolecular compound to approach the active centre. Thus, with two methyls, 4,6-DMDBT showed the lowest sulfur removal, in spite of owning the highest electron density. Meanwhile, for DT was with the longer alkyl chain, the desulfurization efficiency was lower than that of DBT. Therefore, the reactivity of sulfur removal decreased in the order of DBT > DT > BT > 4,6-DMDBT.

Recycling experiments

The reusability of the [pmim]$FeCl_4$-MCM-41 catalyst was investigated on the removal of DBT in ECODS system. When the reaction was finished, the upper layer oil was decanted and recharged with fresh oil and oxidant. The sulfur removal was 91.6, 89.7, 88.3, and 86.1% for the first time to the fourth time, respectively. According to our observation, more and more DBT sulfone was produced in the IL, as the recycle times increased. So it may lead to the slight decrease of catalytic activity in the recycles. Through FTIR analysis, a fresh catalyst and a recycled catalyst exhibited almost the same structure, indicating that [pmim]$FeCl_4$-MCM-41 was a durable catalyst.

Table 4. Variation of Molar Ratio of [pmim]Cl to $FeCl_3$ in the Desulfurization System on Removal of DBT

Entry	n([pmim]Cl: $FeCl_3$)	Sulfur Removal[a] (%)
1	1:1	86.8
2	1:1.5	91.6
3	1:2	91.8
4	1:3	92.7

Experimental conditions: 5-mL model oil, 0.06-g catalyst, 0.39-mmol H_2O_2, 1-mL [Omim]BF_4, 30°C, 1 h.
[a] Max error = ±3%.

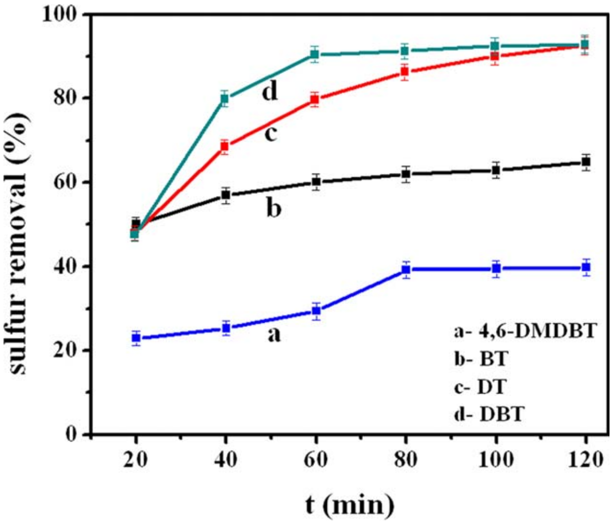

Figure 7. The effect of sulfur species on sulfur conversion.

Experimental conditions: 5-mL model oil, $n(H_2O_2) = 0.39$ mmol, m([pmim]FeCl$_4$-MCM-41) = 0.06 g, V([Omim]BF$_4$) = 1 mL, $T = 30°C$. [Color figure can be viewed in the online issue, which is available at wileyonlinelibrary.com.]

The process of ECODS

ODS system including [pmim]FeCl$_4$-MCM-41 and H_2O_2 without IL ([Omim]BF$_4$), showed much lower desulfurization efficiency (sulfur removal only reached 11.8%). It was illustrated that oxidizing reaction hardly proceeded in oil phase. When the extractant [Omim]BF$_4$ was added into the aforementioned reaction system, the removal of DBT increased sharply and reached 91.6%. During this process, with rigorous stirring DBT was first extracted into ionic liquid phase from oil phase, then was catalyzed, and oxidized by dispersing catalyst and hydrogen peroxide in ionic liquid phase. In this process, [Omim]BF$_4$ not only served as the extractant and the reaction media but also could prevent H_2O_2 from decomposing to some extent. After the reaction, the lower layer IL phase was separated and extracted by tetrachloromethane at room-temperature. Then, the tetrachloromethane phase and the upper layer oil were analyzed by the GC-MS (Figure 8 and 9). In both the oil phase and tetrachloromethane phase, two main compounds were detected by GC-MS analysis. The species A and B in IL phase match those of DBT and DBTO$_2$, respectively. Although two compounds in the oil phase were just DBT and tetradecane (internal standard substance), in which DBTO$_2$ was not discovered. This result further proved the process of ECODS. As the product of DBT oxidation, DBTO$_2$ accumulated in IL phase, which was easily separated from the IL phase. The plausible extraction and catalytic oxidative mechanism of DBT is shown in Scheme 2.

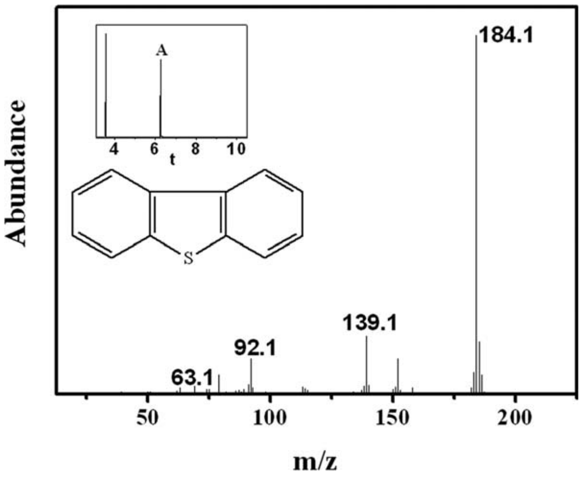

Figure 8. The GC-MS of main compounds of the oil phase.

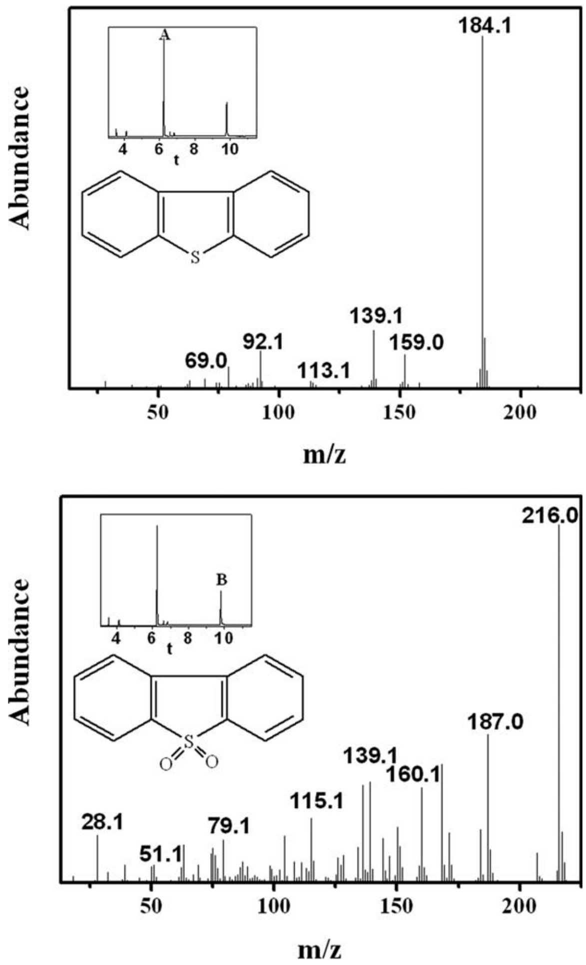

Figure 9. The GC-MS of main compounds of the IL phase.

S2

Conclusions

In conclusion, the mesoporous material MCM-41-supported Fenton-like ionic liquid has been successfully prepared and applied in catalytic ODS. The Fenton-like ionic liquid was incorporated into MCM-41 via the grafting method. The low-angle XRD and N_2 adsorption-desorption revealed that MCM-41-supported Fenton-like ionic liquid remained the mesoporous structure of MCM-41. Among the different desulfurization systems, the ECODS system containing [pmim]FeCl$_4$-MCM-41, H_2O_2, and [Omim]BF$_4$ showed the highest catalytic activity. The catalytic oxidation reaction of sulfur-containing compounds decreased in the order of DBT > DT > BT > 4,6-DMDBT. Through the GC-MS analysis, DBTO$_2$ was confirmed to be the only product of DBT oxidizing reaction and the produce accumulated in

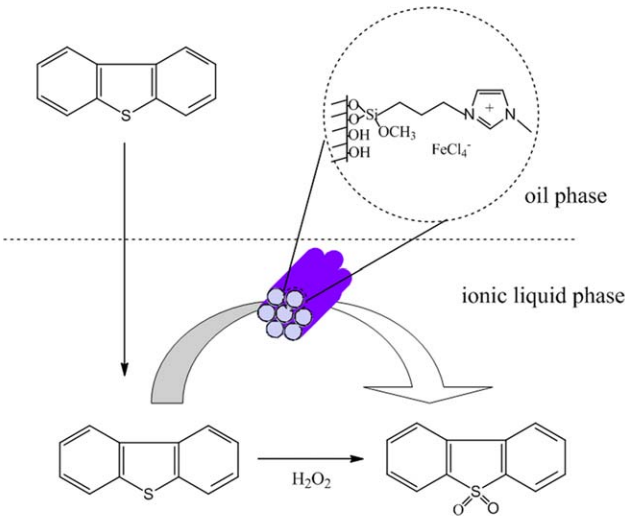

Scheme 2. Oxidation of DBT to $DBTO_2$ in presence of [pmim]$FeCl_4$-MCM-41 as a catalyst.

[Color figure can be viewed in the online issue, which is available at wileyonlinelibrary.com.]

the IL phase. The precipitated sulfones and clean oil could be separated easily.

Acknowledgements

This work was financially supported by the National Nature Science Foundation of China (Nos. 21106055, 21266007, 21076099, 21106057), Specialized Research Fund for the Doctoral Program of Higher Education of China (No. 20103227110016), The Natural Science Foundation of Jiangsu Province (No. BK2011506), and by State Key Laboratory of Heavy Oil Processing.

Literature Cited

1. Yan XM, Mie P, Lei JH, Mi YZ, Xiong L, Guo LP. Synthesis and characterization of mesoporous phosphotungstic acid/TiO_2 nanocomposite as a novel oxidative desulfurization catalyst. *J Mol Catal A: Chem.* 2009;304:52–57.
2. Kwak C, Lee JJ, Bae JS, Choi K, Moon SH. Hydrodesulfurization of DBT, 4-MDBT, and 4,6-DMDBT on fluorinated CoMoS/Al_2O_3 catalysts. *Appl Catal A: Gen.* 2000;200:233–242.
3. Hermann N, Brorson M, Topsøe H. Activities of unsupported second transition series metal sulfides for hydrodesulfurization of sterically hindered 4,6-dimethyldibenzothiophene and of unsubstituted dibenzothiophene. *Catal Lett.* 2000;65:169–174.
4. Bösmann A, Datsevich L, Jess A, Lauter A, Schmitz C, Wasserscheid P. Deep desulfurization of diesel fuel by extraction with ionic liquids. *Chem Commun.* 2001;2494–2495.
5. Eßer J, Wasserscheid P, Jess A. Deep desulfurization of oil refinery streams by extraction with ionic liquids. *Green Chem.* 2004;6:316–322.
6. Kuhlmann E, Haumann M, Jess A, Seeberger A, Wasserscheid P. Ionic liquids in refinery desulfurization: comparison between biphasic and supported ionic liquid phase suspension processes. *ChemSusChem.* 2009;2:969–977.
7. Yang HY, Tatarchuk B. Novel-doped zinc oxide sorbents for low temperature regenerable desulfurization applications. *AIChE J.* 2010; 56:2898–2904.
8. Wang SQ, Zhou L, Su W, Sun Y, Zhou YP. Deep desulfurization of transportation fuels by characteristic reaction resided in adsorbents. *AIChE J.* 2009;55:1872–1881.
9. Li WL, Tang H, Zhang T, Li Q, Xing JM, Liu HZ. Ultra-deep desulfurization adsorbents for hydrotreated diesel with magnetic mesoporous aluminosilicates. *AIChE J.* 2010;56:1391–1396.
10. Lo WH, Yang HY, Wei GT. One-pot desulfurization of light oils by chemical oxidation and solvent extraction with room temperature ionic liquids. *Green Chem.* 2003;5:639–642.
11. Lu Y, Wang Y, Gao LD, Chen JC, Mao JP, Xue QS, Liu Y, Wu HH, Gao GH, He MY. Aerobic oxidative desulfurization: a promising approach for sulfur removal from fuels. *ChemSusChem.* 2008;1: 302–306.
12. Gao GH, Cheng SF, An Y, Si XJ, Fu XL, Liu YM, Zhang HJ, Wu P, He MY. Oxidative desulfurization of aromatic sulfur compounds over titanosilicates. *ChemCatChem.* 2010;2:459–466.
13. Kim TW, Kim MJ, Kleitz F, Nair MM, Guillet-Nicolas R, Jeong KE, Chae HJ, Kim CU, Jeong SY. Tailor-made mesoporous Ti-SBA-15 catalysts for oxidative desulfurization of refractory aromatic sulfur compounds in transport fuel. *ChemCatChem.* 2012;4:687–697.
14. Soleimani M, Bassi A, Margaritis A. Biodesulfurization of refractory organic sulfur compounds in fossil fuels. *Biotechnol Adv.* 2007;25: 570–596.
15. Kulkarni PS, Afonso CAM. Deep desulfurization of diesel fuel using ionic liquids: current status and future challenges. *Green Chem.* 2010;12:1139–1149.
16. Jiang YQ, Zhu WS, Li HM, Yin S, Liu H, Xie QJ. Oxidative desulfurization of fuels catalyzed by Fenton-like ionic liquids at room temperature. *ChemSusChem.* 2011;4:399–403.
17. Wang WH, Li G, Li WG, Liu LP. Synthesis of hierarchical TS-1 by caramel templating. *Chem Commun.* 2011;47:3529–3531.
18. Yu GR, Zhao JJ, Song DD, Asumana C, Zhang XY, Chen XC. Deep oxidative desulfurization of diesel fuels by acidic ionic liquids. *Ind Eng Chem Res.* 2011;50:11690–11697.
19. Huang D, Wang YJ, Cui YC, Luo GS. Direct synthesis of mesoporous TiO_2 and its catalytic performance in DBT oxidative desulfurization. *Microporous Mesoporous Mater.* 2008;116:378–385.
20. Yang LN, Li J, Yuan XD, Shen J, Qi YT. One step non-hydrodesulfurization of fuel oil: catalyzed oxidation adsorption desulfurization over HPWA-SBA-15. *J Mol Catal A: Chem.* 2007; 262:114–118.
21. Torres-García E, Canizal G, Velumani S, Ramírez-verduzco LF, Murrieta-Guevara F, Ascencio JA. Influence of surface phenomena in oxidative desulfurization with WOx/ZrO_2 catalysts. *Appl Phys A.* 2004;79:2037–2040.
22. Hasan Z, Jeon J, Jhung SH. Oxidative desulfurization of benzothiophene and thiophene with WOx/ZrO_2 catalysts: effect of calcination temperature of catalysts. *J Hazard Mater.* 2012;205-206:216–221.
23. Li BS, Ma W, Liu JJ, Han CY, Zuo SL, Li XF. Synthesis of the well-ordered hexagonal mesoporous silicate incorporated with phosphotungstic acid through a novel method and its catalytic performance on the oxidative desulfurization reaction. *Catal Commun.* 2011; 13:101–105.
24. Li BS, Liu ZX, Han CY, Liu JJ, Zuo SL, Zhou ZY, Pang XM. Preparation, characterization and catalytic performance of the silica pillared clay incorporated with phosphotungstic acid using different surfactants as template. *J Mol Catal A: Chem.* 2011;348:106–113.
25. Li BS, Liu ZX, Liu JJ, Zhou ZY, Gao XH, Pang XM, Sheng HT, Preparation, characterization and application in deep catalytic ODS of the mesoporous silica pillared clay incorporated with phosphotungstic acid. *J Colloid Interface Sci.* 2011;362:450–456.
26. Shah AT, Li BS, Abdall ZEA. Direct synthesis of Ti-containing SBA-16-type mesoporous material by the evaporation-induced self-assembly method and its catalytic performance for oxidative desulfurization. *J. Colloid Interface Sci.* 2009;336:707–711.
27. Li BS, Wu K, Yuan TH, Han CY, Xu JQ, Pang XM. Synthesis, characterization and catalytic performance of high iron content mesoporous Fe-MCM-41. *Microporous Mesoporous Mater.* 2012;151: 277–281.
28. Yan XM, Mei P, Lei JH, Mi YZ, Xiong L, Guo LP. Synthesis and characterization of mesoporous phosphotungstic acid/TiO_2 nanocomposite as a novel oxidative desulfurization catalyst. *J Mol Catal A: Chem.* 2009;304:52–57.
29. Li HM, Zhu WS, Wang Y, Zhang JT, Lu JD, Yan YS. Deep oxidative desulfurization of fuels in redox ionic liquids based on iron chloride. *Green Chem.* 2009;11:810–815.
30. Zhu WS, Zhang JT, Li HM, Chao YH, Jiang W, Yin S, Liu H. Fenton-like ionic liquids/H_2O_2 system: one-pot extraction combined with oxidation desulfurization of fuel. *RSC Adv.* 2012;2:658–664.
31. Zhu WS, Zhu GP, Li HM, Chao YH, Chang YH, Chen GY, Han CR. Oxidative desulfurization of fuel catalyzed by metal-based surfactant-type ionic liquids. *J Mol Catal A: Chem.* 2011;347:8–14.

32. Huang WL, Zhu WS, Li HM, Shi H, Zhu GP, Liu H, Chen GY. Heteropolyanion-based ionic liquid for deep desulfurization of fuels in ionic liquids. *Ind Eng Chem Res.* 2010;49:8998–9003.
33. Zhu WS, Huang WL, Li HM, Zhang M, Jiang W, Chen GY, Han CR. Polyoxometalate-based ionic liquids as catalysts for deep desulfurization of fuels. *Fuel Process Technol.* 2011;92:1842–1848.
34. Gao HS, Guo C, Xing JM, Zhao JM, Liu HZ. Extraction and oxidative desulfurization of diesel fuel catalyzed by a Brønsted acidic ionic liquid at room temperature. *Green Chem.* 2010;12:1220–1224.
35. Zhao DS, Wang JL, Zhou EP. Oxidative desulfurization of diesel fuel using a Brønsted acid room temperature ionic liquid in the presence of H_2O_2. *Green Chem.* 2007;9:1219–1222.
36. Li FT, Kou CG, Sun ZM, Hao YJ, Liu RH, Zhao DS. Deep extractive and oxidative desulfurization of dibenzothiophene with $C_5H_9NO{\cdot}SnCl_2$ coordinated ionic liquid. *J Hazard Mater.* 2012;205-206:164–170.
37. Grün M, Unger KK, Matsumoto A, Tsutsumi K. Novel pathways for the preparation of mesoporous MCM-41 materials: control of porosity and morphology. *Microporous Mesoporous Mater.* 1999;27:207–216.
38. Sun JH, Shan ZP, Maschmeyer T, Moulijn JA, Coppens MO. Synthesis of tailored bimodal mesoporous materials with independent control of the dual pore size distribution. *Chem Commun.* 2001; 2670–2671.
39. Sun JH, Shan ZP, Maschmeyer T, Coppens M-O. Synthesis of bimodal nanostructured silicas with independently controlled small and large mesopore sizes. *Langmuir.* 2003;19:8395–8402.
40. Wang GJ, Yu NY, Peng L, Tan R, Zhao HH, Yin DH, Qiu HY, Fu ZH, Yin DL. Immobilized chloroferrate ionic liquid: an efficient and reusable catalyst for synthesis of diphenylmethane and its derivatives. *Catal Lett.* 2008;123:252–258.
41. Melero JA, Iglesias J, Arsuaga JM, Sainz-Pardo J, Frutos P. de, Blazquez S. Synthesis, characterization and catalytic activity of highly dispersed Mo-SBA-15. *Appl Catal A: Gen.* 2007;331:84–94.
42. Hulea V, Dumitriu E. Styrene oxidation with H_2O_2 over Ti-containing molecular sieves with MFI, BEA and MCM-41 topologies. *Appl Catal A: Gen.* 2004;277:99–106.
43. Tatsumi T, Koyano KA, Igarashi N. Remarkable activity enhancement by trimethylsilylation in oxidation of alkenes and alkanes with H_2O_2 catalyzed by titanium-containing mesoporous molecular sieves. *Chem Commun.* 1998;325–326.
44. Chen LY, Chuah GK, Jaenicke S. Propylene epoxidation with hydrogen peroxide catalyzed by molecular sieves containing framework titanium. *J Mol Catal A: Chem.* 1998;132:281–292.
45. Caero LC, Hernández E, Pedraza F, Murrieta F. Oxidative desulfurization of synthetic diesel using supported catalysts: part I. Study of the operation conditions with a vanadium oxide based catalyst. *Catal Today.* 2005;107-108:564–569.
46. Gao J, Wang JQ, Song QW, He LN. Iron(III)-based ionic liquid-catalyzed regioselective benzylation of arenes and heteroarenes. *Green Chem.* 2011;13:1182–1186.
47. Otsuki S, Nonaka T, Takashima N, Qian WH, Ishihara A, Imai T, Kabe T. Oxidative desulfurization of light gas oil and vacuum gas oil by oxidation and solvent extraction. *Energy Fuels.* 2000;14: 1232–1239.

Manuscript received Aug. 21, 2012, and revision received May 22, 2013.